

MODELING OF THE SEISMIC RESPONSE OF THE AGGREGATE PIER FOUNDATION SYSTEM

Christian H. Girsang¹, Marte S. Gutierrez², Member, ASCE, and
Kord J. Wissmann, P.E.³

ABSTRACT: There are a lot of ground improvement techniques that have been developed. One of them is the aggregate pier foundation system. The response of an aggregate pier foundation system during seismic loading was investigated. Comprehensive numerical modeling using FLAC were performed. The research was divided into three parts: 1) ground acceleration, 2) excess pore water pressure ratio, and 3) shear stress distribution in the soil matrix generated during seismic loading. Two earthquake time histories scaled to different maximum acceleration (pga) were used in the numerical modeling: the 1989 Loma Prieta earthquake (pga = 0.45g) and the 1988 Saguenay earthquake (pga = 0.05g). The results of the simulation showed that: 1) the aggregate pier amplifies the peak horizontal acceleration on the ground surface (a_{max}), 2) the aggregate pier reduces the liquefaction potential up to depth where it is installed, 3) pore pressures are generally lower for soils reinforced with aggregate pier than unreinforced soils, except when the applied shear stresses exceed the cyclic shear resistance of the aggregate materials, and 4) the maximum shear stresses in soil are much smaller for reinforced soils than unreinforced soils.

INTRODUCTION

One of the most dramatic cause of damage of structures during earthquakes is the development of liquefaction in saturated cohesionless deposits. Because of the damages that are caused by liquefaction, specialized construction procedures have

¹ Head of Soil Mechanics Laboratory, Pelita Harapan University, Department of Civil Engineering, UPH Tower, Lippo Karawaci, Tangerang 15811, Banten, Indonesia, c_girsang@yahoo.com

² Associate Professor, Virginia Polytechnic Institute and State University, The Charles E. Via, Jr., Department of Civil and Environmental Engineering, 200 Patton Hall, Blacksburg, VA 24061-0105

³ President, Geopier Foundation Company, Inc., 200 Country Club Drive, Suite D-1, Blacksburg, VA 24060

been developed to reduce them. Various techniques have been developed to densify the liquefiable soil and to provide drainage path to accelerate pore pressure dissipation during seismic loading. Aggregate pier foundation system is one of the examples of ground improvement techniques that have been used to reinforce matrix soils and increase the resistance to liquefaction.

The use of aggregate pier foundation system has been gaining wide acceptance in the past decades. Its capabilities to increase the bearing pressure of weak soil, to reduce settlement, and to provide uplift capacity have been studied extensively (e.g., Lawton and Fox 1994; Fox and Edil 2000). Because of the success of aggregate pier foundation system in improving the static response of foundations, there has been an increasing interest to use aggregate pier to improve the seismic response of ground. The behavior of aggregate piers under seismic loading has been a subject of recent research and is summarized by Lawton and Merry (2000).

The typical construction process of aggregate pier foundation system can be divided into four main stages:

1. A cylindrical or rectangular prismatic (linear) cavity in the soil matrix is created by augering or trenching,
2. Aggregate (clean stone) is placed at the bottom of cavity,
3. A bottom bulb is constructed by ramming the aggregate with tamper, which has 45° beveled foot, and
4. The shaft is constructed with undulating layers in thin lifts (30 cm or less) consisting of well-graded or open-graded aggregate, typically stone as used for highway base course material.

NUMERICAL MODELING

Comprehensive numerical modeling using FLAC (FLAC 2000), a finite difference computer code, were performed. For this research, the matrix soil was modeled as an elasto-plastic material with a Mohr-Coulomb failure criterion. The Mohr-Coulomb criterion incorporates dilation at failure but not densification during cyclic loading at stress below failure. Modification of the Mohr-Coulomb model was done to simulate volumetric strains in drained cyclic loading or pore pressures in undrained cyclic loading. The changes in volumetric strains or pore pressures were modeled using the Finn model (Martin et al. 1975). The aggregate pier was represented by elements in the FLAC grids that were assigned a Mohr Coulomb response without including the Finn model modification.

In dynamic analyses, the silent boundaries and free field boundaries (FLAC 2000) were applied so that the outward waves propagating from inside the model may be properly absorbed by the side boundaries.

Figures 1 and 2 show the grid generation used in the numerical model. The darker color indicates the aggregate pier elements and the lighter color shows the soil elements. The models simulate reinforced “cells” of soil that are 2.5 m wide with two different heights: 4.5 m for Figure 1 and 8 m for Figure 2.

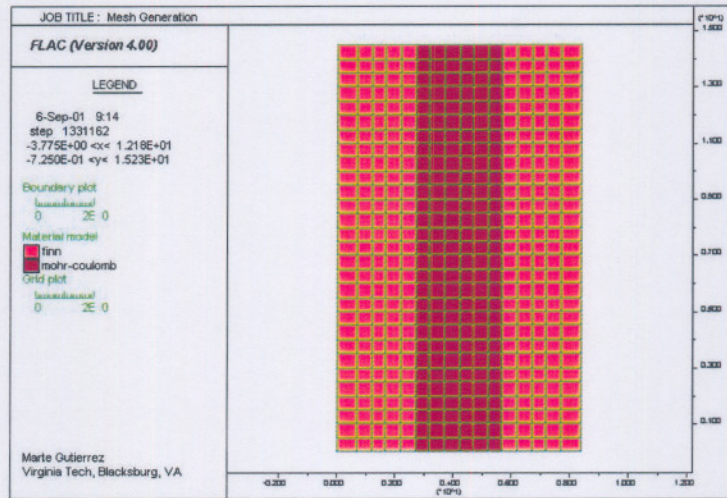


FIG. 1. Grid generation 1

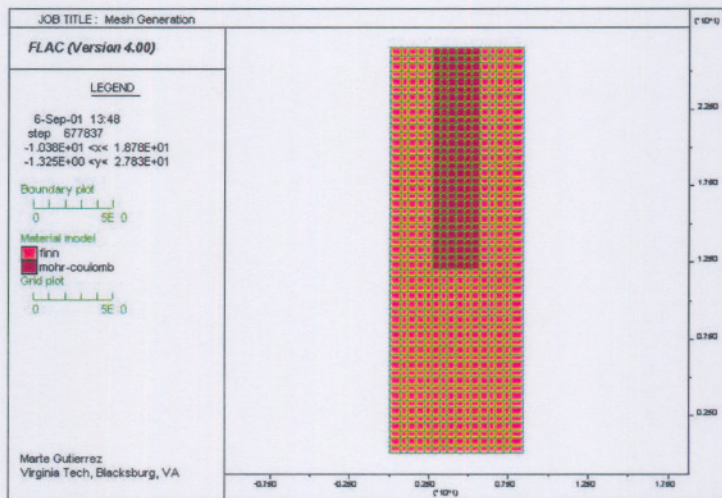


FIG. 2. Grid generation 2

The following strong motions from two earthquakes were used in the numerical modeling:

1. The 17 October 1989 Loma Prieta earthquake as recorded at Corralitos station, California with magnitude (M_w) of 7.1 and peak ground acceleration of 0.64g scaled down to 0.45g.
2. The 25 November 1988 Saguenay earthquake as recorded at Chicoutimi-Nord, Quebec with magnitude (M_w) of 6.0 and peak ground acceleration of 0.05g.

Both earthquake records were filtered and baseline corrected following the procedures previously explained using the software Bandpass (Olgun 2001) written in MATLAB version 5.3 (1999).

For the Loma Prieta earthquake records, the model was shaken for 16 seconds. For the Saguenay earthquake, the model was shaken for 13 seconds.

The models that were analyzed using FLAC version 4.0 (FLAC 2000) are shown on Figure 3. The models incorporate the following soil conditions: loose silty sand with 20% fines content (Figures 3a, 3b, 3e, and 3f), silty sand over soft clay (Figures 3c and 3g), and silt (Figures 3d and 3h). Hence, the determination of the soil parameter values is different for each model.

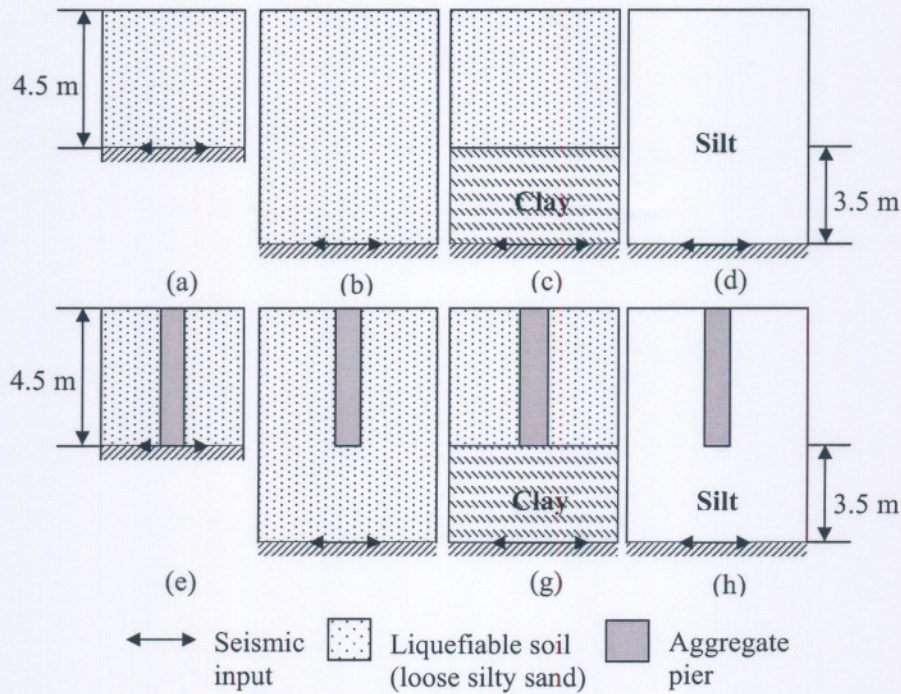


FIG. 3. Models used in FLAC analyses

Table 1 shows the summary of parameters and values that were used in FLAC analyses.

TABLE 1. Summary of parameter values used in FLAC analyses

Parameters (1)	Loose silty sand (2)	Soft clay (3)	Silt (4)	Aggregate pier		Water (7)
				Silty sand ^{a)} (5)	Silt ^{b)} (6)	
Saturated unit weight, γ_{sat} (kN/m ³)	19	17	18	23	23	10
Dry unit weight, γ_d (kN/m ³)	15	12	13	21	21	N/A
Young's modulus, E (kPa)	15080	5030	10055	44700	29800	N/A
Bulk modulus, K (kPa)	15080	9790	12510	24000	16000	10 ⁻⁷
Shear modulus, G (kPa)	5655	1780	3680	18790	12525	N/A
Cohesion, c (kPa)	0	10	3	0	0	N/A
Friction angle, ϕ (°)	30	17	25	50	50	N/A
Dilation angle, ψ (°)	0	0	0	0	0	N/A
SPT (N ₁) ₆₀ (blows/30 cm)	10	4	8	N/A	N/A	N/A
Void ratio, e	0.7	1.1	0.9	0.25	0.25	N/A
Porosity, n	0.412	0.524	0.474	0.2	0.2	N/A
Permeability, k (cm/sec)	10 ⁻⁴	10 ⁻⁷	10 ⁻⁶	10 ⁻¹	10 ⁻¹	N/A

^{a)} Aggregate pier with silty sand as soil matrix

^{b)} Aggregate pier with silt as soil matrix

INTERPRETATION OF RESULTS OF NUMERICAL ANALYSES

There were total of 20 cases analyzed using FLAC. The Loma Prieta and Saguenay earthquake records were used to analyze 9 cases each as shown on Table 2 and Figure 3. Cases with C indicate cases using Loma Prieta earthquake and cases with S indicate cases using Saguenay earthquake. The last two cases were analyzed with emphasis on the shear stress in soil matrix using the Loma Prieta earthquake records.

TABLE 2. Analyses using FLAC

Case no. (1)	Figures used in FLAC (2)	Case no. (3)	Figures used in FLAC (4)
1C	Figure 3(a)	1S	Figure 3(a)
2C	Figure 3(e)	2S	Figure 3(e)
3C	Figure 3(b)	3S	Figure 3(b)
4C	Figure 3(f)	4S	Figure 3(f)
5C	Figure 3(c)	5S	Figure 3(c)
6C	Figure 3(g)	6S	Figure 3(g)
7C	Figure 3(d)	7S	Figure 3(d)
8C	Figure 3(h)	8S	Figure 3(h)
9C	Figure 3(f) with drainage allowed	9S	Figure 3(f) with drainage allowed
1C2	Figure 3(a)	2C2	Figure 3(e)

The following sections discuss the results of the numerical analyses.

Ground Acceleration

The installation of aggregate pier amplifies the ground motions (a_{max}) when subjected to seismic loading. This is because the aggregate piers stiffen the system. Table 3 summarizes the values of a_{max} . Note that the peak acceleration on rock outcrops is designated as pga and the peak acceleration at the soil surface is designated as a_{max} . Table 3 shows that the input ground acceleration (pga) is de-amplified for cases with Loma Prieta earthquake and is amplified for cases with Saguenay earthquake except for cases with silty sand layer underlain by soft clay, namely Cases 5S and 6S.

TABLE 3. Values of ground acceleration from FLAC analyses

Case (1)	pga (2)	a_{max} (3)	Note (4)	Case (5)	pga (6)	a_{max} (7)	Note (8)
1C	0.45g	0.163g	D	1S	0.05g	0.086g	A
2C	0.45g	0.381g	D	2S	0.05g	0.100g	A
3C	0.45g	0.155g	D	3S	0.05g	0.059g	A
4C	0.45g	0.380g	D	4S	0.05g	0.098g	A
5C	0.45g	0.134g	D	5S	0.05g	0.0384g	D
6C	0.45g	0.419g	D	6S	0.05g	0.040g	D
7C	0.45g	0.269g	D	7S	0.05g	0.0562g	A
8C	0.45g	0.416g	D	8S	0.05g	0.0616g	A
9C	0.45g	0.433g	D	9S	0.05g	0.0993g	A

(Note: D = Deamplification; A = Amplification)

It is apparent that the use of aggregate pier amplifies the ground acceleration (a_{max}) by a factor ranging from 1.55 to 3.13 for the Loma Prieta earthquake and 1.04 to 1.67 for the Saguenay earthquake. The average value for both earthquake ranges from 1.4 to 2.3. This phenomenon is not surprising and has been shown by other researchers, for example by Liu and Dobry (1997). Liu and Dobry (1997) studied a model of footing and showed that the amplification ratios of the footing resting on compacted sand zone within a liquefiable soil mass increase as the depth of the compacted zone increases.

Excess Pore Water Pressure Ratio

The second parameter that will be discussed in this section is the excess pore water pressure ratio (r_u). The excess pore water pressure ratio (r_u) is defined as the ratio between excess pore water pressure and the initial effective vertical stress. The r_u values discussed here are the peak values.

The peak values of r_u were collected and compared between cases with and without aggregate piers to observe the degree of improvement that occurs by installing aggregate piers as shown on Figure 4. A best-fit curve was plotted as indicated by the solid line.

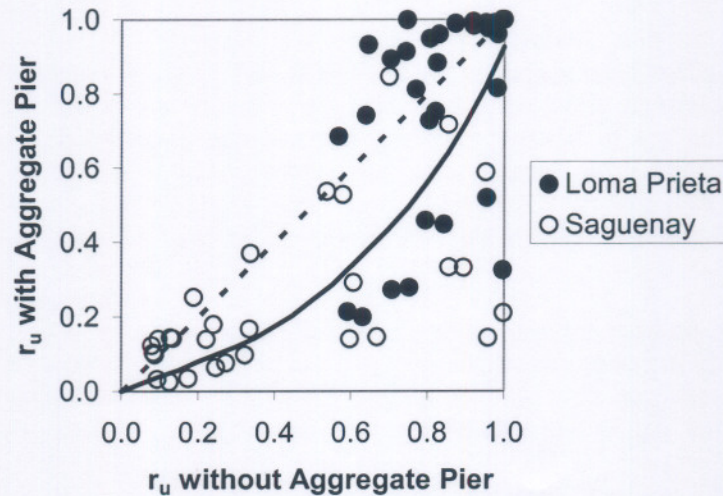


FIG. 4. Comparison of peak values of r_u between cases with and without aggregate pier for Loma Prieta and Saguenay earthquakes

From Figure 4 it is apparent that for Loma Prieta earthquake most of the data points actually lay above the 1:1 line indicated by the dashed line. It means that most r_u values increase due to the installation of aggregate pier. It appears that for cases where the input acceleration (pga) overcomes the shear strength of the reinforced soil, no reduction in r_u value is obtained.

Figure 4 also shows that for Saguenay earthquake most of the data points lay beneath the 1:1 line (the dashed line). It means that for Saguenay earthquake most r_u values decrease due to the installation of aggregate piers.

Since Figure 4 shows that most data points lie beneath the 1:1 line, it can be generally concluded that improvement occurs due to the installation of aggregate pier. Note that improvement is defined as a decrease in the values of r_u as a result of the installation of aggregate pier.

Shear Stress in Soil Matrix

In the Simplified Procedure proposed by Seed and Idriss (1971), the maximum shear stress in soil matrix (τ_{max}) can be estimated by multiplying the stress reduction coefficient (r_d), total overburden pressure (σ_0), and the peak horizontal acceleration at the ground surface (a_{max}) as shown in (1).

$$\tau_{max} = r_d * \sigma_0 * \frac{a_{max}}{g} \quad (1)$$

Baez and Martin (1993) and Goughnour and Pestana (1998) introduced a new parameter, which they defined as the shear stress reduction factor (K_G), as shown on eqs. 2 and 3, respectively.

$$K_G = \frac{\tau_s}{\tau} = \frac{1}{1 + R_a(R_s - 1)} \quad (2)$$

$$K_G = \frac{\tau_s}{\tau} = \frac{1 + R_a(n - 1)}{1 + R_a(R_s - 1)} \quad (3)$$

where:

τ_s = shear stress in the soil matrix

τ = the input shear stress

n = the vertical stress ratio which is the ratio of the effective overburden pressure within the stone column to the effective overburden pressure within the soil matrix. The value of n varies between 4 and 10 based on model tests and 2 to >10 based on field measurement.

The ratio between the area of reinforcing element and the total plan area can be written as $R_a = A_r/A$ and the ratio between the shear modulus of the reinforcing element and the shear modulus of the soil can be written as $R_s = G_r/G_s$.

The shear stress in soil matrix (τ_s) can be estimated by multiplying K_G with the average shear stress (τ_{ave}) calculated using the following equation:

$$\tau_{ave} = 0.65 * \sigma_0 * \frac{a_{max}}{g} * r_d \quad (4)$$

Eq. 4 can be written in terms of maximum shear stress (τ_{max}), which is shown by (1). Hence, (2) can also be written in terms of maximum shear stress (τ_{max}).

$$K_G = \frac{\tau_s}{\sigma_0 \frac{a_{max}}{g} r_d} \quad (5)$$

By applying values of τ_{max} calculated using FLAC into (5), the values of K_G can be calculated. This procedure was applied to the case with aggregate pier (Case 2C2) with value of a_{max} of 0.37g. Figure 5 shows plot of average K_G values versus depth. It can be seen that the average value of K_G is 0.17 throughout all depths.

The values of K_G calculated using (5) were based on shear stress calculated using the Simplified Procedure (Seed and Idriss 1971), which does not take into account the effects of reinforcing elements. To overcome this problem a modification to the shear stress reduction factor (K_G) is introduced, the shear stress reduction factor, which takes into account the reinforcement factor (K_{GR}). The value of K_{GR} is nothing

more than the ratio of the maximum shear stress for cases with aggregate pier to cases without aggregate pier obtained from FLAC analyses.

$$K_{GR} = \frac{(\tau_{\max})_{\text{with aggregate pier}}}{(\tau_{\max})_{\text{without aggregate pier}}} \quad (6)$$

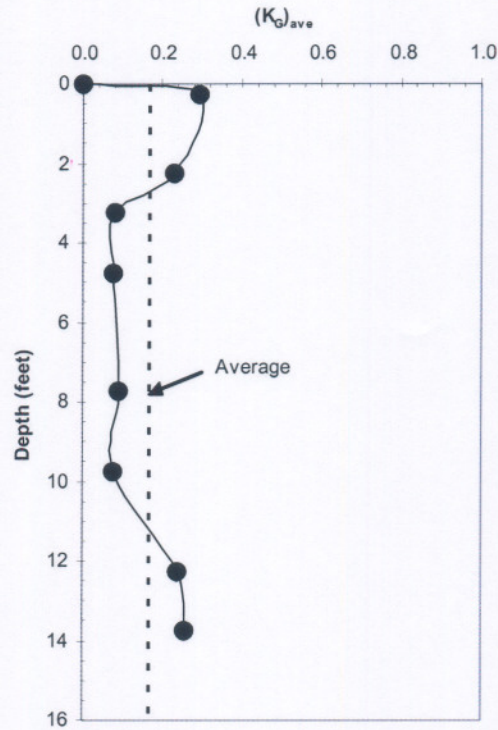


FIG. 5. Plot of values of $(K_G)_{\text{ave}}$ versus depths for Case 2C2

To make the discussion easier, the case analyzed was given a new name. Case C2 represents the ratio of Case 2C2 and Case 1C2 in (6).

Figure 6 shows plot of average K_{GR} values versus depth. It is apparent that the K_{GR} values in the aggregate pier are much larger than those in the soil matrix. This shows that the aggregate pier carries more shear stresses than the soil matrix under seismic loading. From Figure 6, it can be seen that the average values of K_{GR} are approximately 0.6 and 3.6 for the soil matrix and the aggregate pier, respectively.

It can be concluded that the average value of K_{GR} for matrix soil (0.6) is much larger than the value of K_G of 0.17 for Case 2C2. It is apparent that the value of K_G calculated using (5) gives smaller value than the value of K_{GR} calculated using (6). The use of K_{GR} value is more preferable since it depicts the “real” reinforcing effects of aggregate pier as shown in (6).

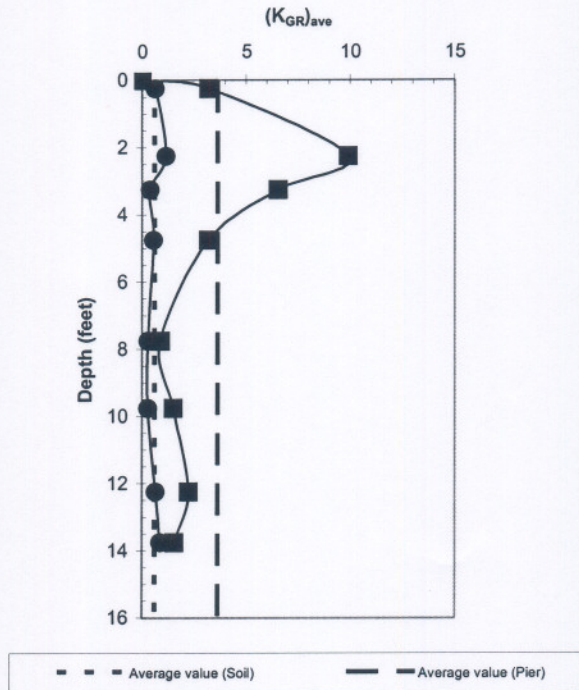


FIG. 6. Plot of values of $(K_{GR})_{ave}$ versus depths for Case C2

A general procedure should be developed to estimate the value of K_{GR} . For this purpose, the procedures proposed by Baez and Martin (1993) and Goughnour and Pestana (1998) were reviewed. Using the procedure proposed by Baez and Martin (1993), a value of K_G of 0.6 is calculated using (2). If the procedure proposed by Goughnour and Pestana (1998) is used, a value of K_G of 0.8 is obtained from (3).

It is observed that the value of K_G calculated using the shear reinforcement approach (2) gives the same value as the value of K_{GR} calculated using (6). Therefore, (2) can be used in designing the reinforcing effects of aggregate pier foundation system during seismic loading.

Figure 7 presents (2) in form of a chart. It is apparent that at any given R_a , the reinforcement factor (K_{GR}) decreases with increasing shear modulus ratio (R_s). It can also be seen that at any given R_s , the reinforcement factor (K_{GR}) decreases with increasing area replacement ratio (R_a).

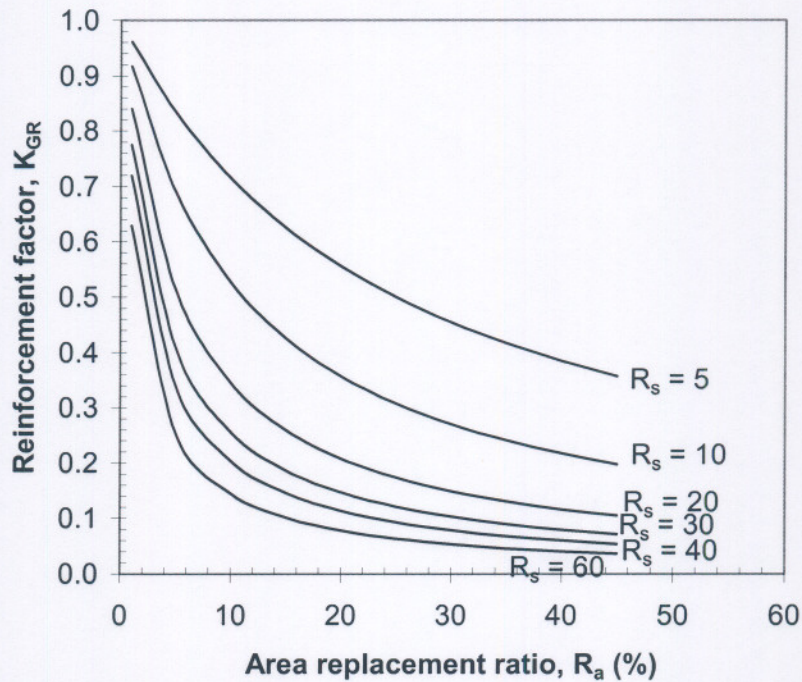


FIG. 7. The reinforcement factor, K_{GR} (after Baez and Martin 1993)

CONCLUSIONS

- The use of aggregate pier generally amplifies the ground acceleration (a_{max}). The input acceleration time history (pga) is amplified for cases with Loma Prieta earthquake. The values of pga are amplified for cases with Saguenay earthquake, except for cases with the presence of soft clay underlying the silty sand layer.
- The effects of installation aggregate pier are much more significant in cases with Saguenay time history. It can be concluded that generally improvement occurs due to the installation of aggregate pier.
- The values of K_G can be estimated by applying values of τ_{max} calculated using FLAC. It can be concluded that the K_G values in the aggregate pier are larger than those in the soil matrix. This shows that the installation of aggregate pier is effective in that the aggregate pier carries more shear stresses than the soil matrix under seismic loading.
- A modification to the shear stress reduction factor (K_G) was introduced that is the shear stress reduction factor, which takes into account the reinforcement factor (K_{GR}). The K_{GR} values in the aggregate pier are much larger than those in the soil matrix. This again shows that the aggregate pier carries more shear stresses than the soil matrix under seismic loading.
- The value of K_G calculated based on shear stresses from FLAC normalized by shear stresses from the Simplified Procedure is smaller than the value of K_{GR} .

The use of K_{GR} value is more preferable since it depicts the “real” reinforcing effects of aggregate pier.

- The equation using the shear reinforcement approach (Eq. 2) agrees well with the value of K_{GR} calculated using FLAC. The equation proposed by Goughnour and Pestana (1998) overestimates the value of K_{GR} .

REFERENCES

Baez, J. I. and Martin, G. R. (1993). “Advances in the design of vibro systems for the improvement of liquefaction resistance”, *Proc. 7th Annual Symp. of Ground Improvement*, 1-16.

FLAC User's Manual – version 4.0. (2000). Itasca Consulting Group, Inc., Minneapolis, Minnesota.

Fox, N. S. and Edil, T. B. (2000). “Case histories of rammed aggregate pier soil reinforcement construction over peat and highly organic soils”, *Proc. Soft Ground Technology*, 146-157.

Goughnour, R. R. and Pestana, J. M. (1998). “Mechanical behavior of stone columns under seismic loading”, *Proc. 2nd Int. Conf. on Ground Improvement Techniques*, 157-162.

Lawton, E. C. and Fox, N. S. (1994). “Settlement of structures supported on marginal or inadequate soils stiffened with short aggregate piers”, *Vertical and Horizontal Deformations of Foundations and Embankments*, Yeung, A. T. and Felio, G. Y., eds., ASCE, GSP No. 40, 2, 962-974.

Lawton, E. C. and Merry, S. M. (2000). “Performance of geopier-supported foundations during simulated seismic tests on Northbound Interstate 15 bridge over South Temple, Salt Lake City, Utah”, Final Report, *Rep. No. UUCVEEN 00-03*, Univ. of Utah, Salt Lake City, Utah, 73pp.

Liu, L. and Dobry, R. (1997). “Seismic response of shallow foundation on liquefiable sand”, *J. Geotech. and Geoenv. Engrg.*, ASCE, 123(6), 557-567.

Martin, G. R., Finn, W. D. L., and Seed, H. B. (1975). “Fundamentals of liquefaction under cyclic loading”, *J. Geotech. Engrg. Div.*, ASCE, 101(GT5), 423-438.

Olgun, C. G. (2001). “Bandpass – Software to process earthquake time histories”, Earthquake Center of Southeastern of United States (ECSUS), Virginia Tech, Blacksburg, Virginia.

Seed, H. B. and Idriss, I. M. (1971). “Simplified procedure for evaluating soil liquefaction potential”, *J. Soil Mech. & Found. Div.*, ASCE, 97(SM9), 1249-1273.